$\eta\gamma$ and $\eta'\gamma$ transition form factors within the running coupling constant method

Shahin S. Agaev
High Energy Physics Laboratory, Baku State University, Z. Khalilov st. 23, 370148 Baku, Azerbaijan
(Received 31 January 2001; published 21 May 2001)

The electromagnetic transition form factors $F_{\eta(\eta')\gamma}(Q^2)$ of the η and η' mesons are calculated within the standard hard scattering approach and the usual η-η' mixing scheme using the running coupling constant method. Power suppressed corrections $\sim 1/Q^p$, $p=2,4,\ldots$ to $Q^2F_{M\gamma}(Q^2)$, are evaluated. On the basis of this analysis deviations of the η_1 and η_8 meson distribution amplitudes (DA's) from the asymptotic form are discussed and model DA's are proposed. In computations as input parameters the phenomenological values of the octet-singlet mixing angle $\theta=-15.4°$ and of the decay constants $f_1\simeq 0.108$ GeV, $f_8\simeq 0.116$ GeV are used. A comparison is made with the experimental data and agreement in a range of the virtuality of the probing photon γ^*, 1.5 GeV$^2 \leqslant Q^2 \leqslant 15$ GeV^2, is found.

DOI: 10.1103/PhysRevD.64.014007 PACS number(s): 12.38.−t, 13.40.Gp, 14.40.Aq

I. INTRODUCTION

One of the important achievements of perturbative QCD (PQCD) is the predictions for certain large-momentum transfer exclusive processes involving hadrons [1–4]. The meson-photon transition form factor (FF) $F_{M\gamma}(Q^2)$ is the simplest such exclusive process. An analysis of the $M\gamma$ transition FF in light-cone perturbation theory, based on light-cone quantization and the light-cone Fock state expansion, was carried out by Brodsky and Lepage [1]. As a result, within the standard hard scattering approach (HSA) the form factor $F_{M\gamma}(Q^2)$ can be expressed as the convolution of the hard scattering amplitude $T_H(x,Q^2;\mu_F^2,\mu_R^2)$ and the process-independent distribution amplitude (DA) $\phi_M(x,\mu_F^2)$ of a corresponding meson. The hard scattering amplitude $T_H(x,Q^2;\mu_F^2,\mu_R^2)$ is calculable within QCD perturbation theory and is known with $O(\alpha_S)$ order accuracy [5–7]. The mesons DA's $\phi_M(x,\mu_F^2)$ are universal functions containing all nonperturbative information on mesonic binding effects and cannot be found by tools of PQCD. Such information must be deduced either from experimental data or from nonperturbative QCD computations [3].

Recently, the CLEO experimental results [8] related with the $\eta\gamma$ and $\eta'\gamma$ transition FF's appeared. To obtain these data various η and η' decay chain analyses, for example, $\eta\to\gamma\gamma$, $\eta\to 3\pi^0$, $\eta'\to\rho^0\gamma\to\pi^+\pi^-\gamma$, were fulfilled. These results and CELLO Collaboration data [9] form the basis for theoretical studies of the $\eta\gamma$, $\eta'\gamma$ transition form factors and the $\eta-\eta'$ mixing problem.

It is known that the physical η and η' states consist dominantly of a flavor SU$_f(3)$ octet η_8 and singlet η_1, respectively. In the usual mixing scheme we have

$$|\eta\rangle = \cos\theta|\eta_8\rangle - \sin\theta|\eta_1\rangle,$$

$$|\eta'\rangle = \sin\theta|\eta_8\rangle + \cos\theta|\eta_1\rangle. \tag{1}$$

The mixing angle θ was extracted from the experimental data [10,11] and was evaluated in various theoretical papers [12–16].

The electromagnetic transition form factors of the η and η' mesons in the light-cone perturbation theory and conventional mixing scheme were computed [13] retaining the dependence of $T_H(x,k_\perp,Q^2)$ on the quark transverse momentum $k_\perp$ and using the spatial wave function $\psi(x,k_\perp)$ modeled in accordance with the Brodsky-Huang-Lepage (BHL) prescription [17]. The numerical results show that there still exists a gap between the data and the light-cone perturbation computation with BHL wave function.

In the modified HSA, in which the transverse degrees of freedom and the Sudakov form factor are taken into account, the $\eta\gamma$ and $\eta'\gamma$ transition FF's were calculated in Ref. [14] and the value $\theta=-18°\pm 2°$ was obtained. The more general mixing scheme with two mixing angles θ_1,θ_8 connecting the decay constants f_1,f_8 of the pseudoscalar mesons η_1,η_8 with the decay constants f_p^i $(i=1,8,\ p=\eta,\eta')$ were also investigated [15,16]. The phenomenological analysis [15] based on the combined analysis of the two-photon decay width of the η and η' mesons, $\eta\gamma$ and $\eta'\gamma$ transition form factors allowed the authors to determine the parameters $\theta_1,\theta_8,f_1,f_8$. The similar analysis [16] was made by expressing η and η' as linear combinations of states η_q and η_s generating by axial vector currents with the flavor structure $q\bar{q}=(u\bar{u}+d\bar{d})/\sqrt{2}$ and $s\bar{s}$, respectively. Again the values of the parameters $\theta_1,\theta_8,f_1,f_8$ as well as the value of the mixing angle of the particle states $\theta=-15.4°$ were found. It is worth noting that works [14,15] applied the modified HSA to calculate the $\eta\gamma$ and $\eta'\gamma$ transition FF's, and for simplicity, the parameters related to transverse degrees of freedom for the mesons η and η' are assumed to be identical and the Gaussian wave function in the transverse part of the wave function is used. The results [14,15] are in good agreement with the data [8].

In this work we shall calculate the $\eta\gamma$ and $\eta'\gamma$ electromagnetic transition form factors within the standard HSA and the conventional mixing scheme using the running coupling constant (RCC) method [18,19]. Computation of the one-loop Feynman diagrams with the running coupling constant $\alpha_S(-k^2)$ at vertices corresponds to calculation of these diagrams by inserting into a gluon line a chain of quark bubbles and allows one to estimate power suppressed (higher twist) corrections to a physical quantity under consideration (see Ref. [18] and references therein). In exclusive processes the coupling constant α_S runs not only due to loop integration, but also because of the integration in the process amplitude over the longitudinal momentum fractions of hadron constituents [19]. Thus the exclusive processes have two independent sources of power corrections to their characteristics; the loop integration and the integration over the longitudinal momentum fractions of quarks and gluons. It is important that the latter source exists even at the leading order of PQCD, when the amplitude of the exclusive process depends on α_S [19,20].

Resummation of $(-\beta_0\alpha_S/4\pi)^n$ corrections to the pion-photon transition FF $F_{\pi\gamma}(Q^2)$, as well as to the Brodsky-Lepage evolution kernel $V[x,y;\alpha_S(Q^2)]$ and to a meson distribution amplitude, has been carried out [21] recently. In this work the authors have also noted the existence of two kinds of power corrections to $F_{\pi\gamma}(Q^2)$: the infrared (IR) renormalon ambiguity arising from the loop integration and power corrections from the regions $x\to 0, x\to 1$. In computation of the transition FF's $F_{\eta\gamma}(Q^2)$ and $F_{\eta'\gamma}(Q^2)$ using the running coupling constant method we shall restrict ourselves by evaluating power corrections coming from the regions $x\to 0, x\to 1$.

This paper is structured as follows: In Sec. II a pseudoscalar meson-photon electromagnetic transition FF $F_{M\gamma}(Q^2)$ in the standard HSA and a meson DA are described. The form factor $F_{M\gamma}(Q^2)$ within the running coupling constant method is considered in Sec. III. Our numerical results for the form factors $F_{\eta\gamma}(Q^2), F_{\eta'\gamma}(Q^2)$ in the usual $\eta-\eta'$ mixing scheme are presented in Sec. IV. Section V contains concluding remarks.

II. PSEUDOSCALAR MESON-PHOTON ELECTROMAGNETIC TRANSITION FORM FACTOR

In this section we consider the $SU_f(3)$ singlet η_1 and octet η_8 mesons electromagnetic transition FF's and their DA's in QCD perturbation theory. Unlike the η_8 meson, the $SU_f(3)$ singlet η_1 contains a two-gluon valence Fock state [22]. This gluonic state at the leading order does not contribute to the form factor $F_{\eta_1\gamma}(Q^2)$, but affects the higher-order corrections to $F_{\eta_1\gamma}(Q^2)$. Owing to the quark-gluon mixing, the gluonic component of the meson DA has an influence also on the evolution of the quark component of the distribution amplitude. But the phenomenological analysis demonstrated [14] that the gluonic admixture to the η_1 meson is small. Therefore in this work we neglect the gluonic part of the meson η_1 distribution amplitude, treating the η_1 and η_8 mesons on the same footing, i.e., as the mesons consisting only on quark valence Fock states.

In the framework of the standard HSA the pseudoscalar meson-photon electromagnetic transition form factor $F_{M\gamma}(Q^2)$ is given by the expression [1]

$$F_{M\gamma}(Q^2)=\int_0^1 dx\ \phi_M(x,\mu_F^2)T_H(x,Q^2;\mu_F^2,\mu_R^2), \qquad (2)$$

where $Q^2=-q^2>0$ and q is the four-momentum of the virtual photon. Here $T_H(x,Q^2;\mu_F^2,\mu_R^2)$ is the hard scattering amplitude of the subprocess $\gamma^*+\gamma\to q+\overline{q}$, $\phi_M(x,\mu_F^2)$ is the meson distribution amplitude. In Eq. (2) μ_F^2 and μ_R^2 represent the factorization and renormalization scales, respectively.

At the leading order the hard scattering subprocess $\gamma^*+\gamma\to q+\overline{q}$ is the pure electromagnetic process and $T_H^0(x,Q^2)$ therefore does not depend on the scales μ_F^2,μ_R^2 and has the following form:

$$T_H^0(x,Q^2)=\frac{N}{Q^2}\left(\frac{1}{x}+\frac{1}{1-x}\right). \qquad (3)$$

The normalization constants N_1 and N_8 for the mesons $\eta_1$and η_8 are given by the formulas

$$N_1=2\sqrt{2}(e_u^2+e_d^2+e_s^2),\quad N_8=2(e_u^2+e_d^2-2e_s^2), \qquad (4)$$

where e_q is the charge of the quark q.

The one-loop QCD correction to the hard scattering amplitude T_H generates its explicit dependence on the scales μ_F^2 and μ_R^2 [5–7]. For the factorization scale μ_F^2 the natural and traditional choice is $\mu_F^2=Q^2$. After choosing $\mu_F^2=Q^2$ and keeping the dependence of T_H on the renormalization scale μ_R^2 [6,7] we get

$$T_H(x,Q^2,\alpha_S)=\frac{N}{Q^2}\frac{1}{x}\left\{1+C_F\frac{\alpha_S(\mu_R^2)}{4\pi}\left[\ln^2 x-\frac{x\ln x}{1-x}-9-\ln\left(\frac{Q^2}{\mu_R^2}\right)\right]\right\}+[x\leftrightarrow(1-x);\ \ \mu_R^2\to\overline{\mu}_R^2]. \qquad (5)$$

If we take in Eq. (5) $\mu_R^2\equiv\overline{\mu}_R^2=Q^2$ we obtain the Braaten's result (3.12) from Ref. [6] (there one has to equal the factorization scale μ to Q and take $\delta=1$).

The proper choice of the renormalization scale $\mu_R^2(\overline{\mu}_R^2)$ is one of the important problems in the QCD perturbation theory [23]. The good choice of μ_R^2 is one that minimizes the higher-order corrections to a physical quantity under question. For physical quantities, which at the leading order of PQCD depend on $\alpha_S(\mu_R^2)$, this procedure is quite transparent. Let us clarify this point considering, as an example, the pion electromagnetic form factor $F_\pi(Q^2)$. This FF at the next-to-leading order contains terms proportional to $\ln[Q^2(1-x)(1-y)/\mu_R^2]$ and taking the renormalization scale as $\mu_R^2=Q^2(1-x)(1-y)$ [19], or as $\mu^2=Q^2(1-x)/2$ [20], one can eliminate at least a part of such terms. But crucial for our purposes is the observation that the scale $\mu_R^2=Q^2(1-x)(1-y)$ (or xyQ^2) is equal to the absolute value of the square of the four-momentum of the virtual hard gluon at the leading-order Feynman diagrams for T_H [23]. In the case of the meson-photon transition form factor $O(\alpha_S^2)$ order corrections to T_H are not known. But we can take μ_R^2 (or $\overline{\mu}_R^2$ depending on the Feynman diagram under consideration) equal to the absolute value of the square of the four-momentum of the virtual quark in the corresponding lowest-order Feynman diagram for T_H. Then it is easy to see that

$$\mu_R^2 = Q^2 x, \quad \overline{\mu_R^2} = Q^2(1-x). \tag{6}$$

Such choice of the renormalization scales μ_R^2 and $\overline{\mu_R^2}$ meets also another requirement important for the hard scattering amplitude T_H. Namely, it remains symmetric under $x \leftrightarrow (1-x)$ in the context of the RCC method, which leads together with the symmetry of the meson M ($M=\eta_1,\eta_8$) DA to equal contributions to $F_{M\gamma}(Q^2)$ coming from the two terms in Eq. (5).

The next ingredient to be chosen in Eq. (2) is the meson DA $\phi_M(x,Q^2)$. In general, the meson DA can be expanded over Gegenbauer polynomials $\{C_n^{3/2}(2x-1)\}$ which are the eigenfunctions of the evolution equation for mesons [1,3] and has the following form:

$$\phi_M(x,Q^2) = \phi_{asy}(x) \sum_{n=0}^{\infty} b_n(Q^2) C_n^{3/2}(2x-1),$$

$$b_n(Q^2) = b_n^0 \left[\frac{\alpha_S(Q^2)}{\alpha_S(\mu_0^2)} \right]^{\gamma_n/\beta_0}, \tag{7}$$

where $\phi_{asy}(x)$ is the meson asymptotic DA

$$\phi_{asy}(x) = \sqrt{3} f_M x(1-x). \tag{8}$$

In Eq. (7) the anomalous dimensions $\{\gamma_n\}$ determine the evolution of $\phi_M(x,Q^2)$ on the factorization scale Q^2, μ_0^2 is the normalization point at which the values of the coefficients $\{b_n^0\}$ can be obtained using, for example, the QCD sum-rules method [3]. For both η_1 and η_8 mesons, due to C-invariance the sum in Eq. (7) runs over even $n=0,2,\ldots$. In other words, the η_1 and η_8 mesons DA's are symmetric under $x \leftrightarrow (1-x)$ replacement.

For our purposes it is convenient to rewrite the distribution amplitude in the form

$$\phi_M(x,Q^2) = \phi_{asy}(x) \sum_{n=0}^{\infty} K_n x^n. \tag{9}$$

The new coefficients K_n in Eq. (9) can be found using Eq. (7) and known expressions for $\{C_n^{\lambda}(\xi)\}$ [24].

Unlike the pion, kaon, ρ_L meson there is some information concerning the η_1,η_8 mesons distribution amplitudes in the literature. Therefore our goal in this paper is twofold; not only to explain the experimental data on the $\eta\gamma$ and $\eta'\gamma$ transition form factors by taking into account power corrections $\sim 1/Q^p$, $p=2,4,\ldots$ to $Q^2 F_{\eta(\eta')\gamma}(Q^2)$, but also to estimate within this scheme values of the coefficients b_n^0. In numerical calculations we shall use the asymptotic DA and DA's with small admixture of the Gegenbauer polynomial $C_2^{3/2}(2x-1)$ and shall fix the value of b_2^0.

III. THE FORM FACTOR $F_{M\gamma}(Q^2)$ IN THE FRAMEWORK OF THE RCC METHOD

To compute the meson-photon electromagnetic transition form factor $F_{M\gamma}(Q^2)$ we have to perform the integration over x in Eq. (2). But having inserted explicit expressions of the hard scattering amplitude $T_H(x,Q^2,\alpha_S)$ from Eq. (5) and of the meson DA from Eq. (9) into Eq. (2), one encounters with divergencies in the regions $x\to 1$ and $x \to 0$, because the running coupling constant $\alpha_S(Q^2x)$ (and $\alpha_S[Q^2(1-x)]$) suffers from infrared singularity in $x\to 0$ (and $x \to 1$) limit. Hence the form factor can be found after regularization of $\alpha_S(\mu_R^2)$ in these end-point regions. Such regularization can be carried out with the aid of the renormalization-group equation, that allows one to express the running coupling constant $\alpha_S(\lambda Q^2)$ in terms of $\alpha_S(Q^2)$. The solution of the renormalization-group equation,

$$\frac{\partial \alpha_S(\lambda Q^2)}{\partial \ln \lambda} = -\frac{\beta_0}{4\pi}[\alpha_S(\lambda Q^2)]^2 - \frac{\beta_1}{16\pi^2}[\alpha_S(\lambda Q^2)]^3, \tag{10}$$

obtained by keeping the leading $(\alpha_S \ln \lambda)^k$ and next-to-leading $\alpha_S(\alpha_S \ln\lambda)^{k-1}$ powers of $\ln\lambda$ is [25]

$$\alpha_S(\lambda Q^2) \simeq \frac{\alpha_S}{1+\ln\lambda/t} - \frac{\alpha_S^2 \beta_1}{4\pi\beta_0} \frac{\ln[1+\ln\lambda/t]}{[1+\ln\lambda/t]^2}. \tag{11}$$

In Eqs. (10) and (11) $t = 4\pi/\beta_0 \alpha_S(Q^2)$, and $\alpha_S \equiv \alpha_S(Q^2)$ is the one-loop QCD coupling constant and β_0,β_1 are the QCD beta-function one- and two-loop coefficients, respectively,

$$\alpha_S(\mu^2) = \frac{4\pi}{\beta_0 \ln(\mu^2/\Lambda^2)}, \quad \beta_0 = 11 - \frac{2}{3} n_f,$$

$$\beta_1 = 102 - \frac{38}{3} n_f, \tag{12}$$

where n_f is the number of quark flavors, Λ is the QCD scale parameter $\Lambda = 0.2$ GeV.

Having inserted Eq. (11) into Eq. (5) and after that, Eqs. (5) and (9) into Eq. (2), we obtain the integral which is still divergent, but has now the form suitable for calculation. Using the method described in details in our work [19], this integral may be found as a perturbative series in $\alpha_S(Q^2)$:

$$Q^2 F_{M\gamma}(Q^2) = A + B \sum_{n=1}^{\infty} \left(\frac{\alpha_S(Q^2)}{4\pi} \right)^n \beta_0^{n-1} C_n, \tag{13}$$

where A,B are constants. The coefficients C_n of the series in Eq. (13) demonstrate factorial growth $C_n \sim (n-1)!$ indicating on the IR renormalon nature of divergences in the integral (2) and in the corresponding series in Eq. (13). The convergence radius of such series is zero and its summation should be performed using the Borel integral techniques, i.e., one has to find the Borel transform $B[Q^2 F_{M\gamma}](u)$ of the series [26],

$$B[Q^2F_{M\gamma}](u)=\sum_{n=1}^{\infty}\frac{u^{n-1}}{(n-1)!}C_n, \tag{14}$$

then invert $B[Q^2F_{M\gamma}](u)$ to obtain the resummed expression for $Q^2F_{M\gamma}(Q^2)$. This approach is straightforward but tedious. These intermediate steps can be bypassed by introducing the inverse Laplace transforms [27],

$$\frac{1}{(t+z)^{\nu}}=\frac{1}{\Gamma(\nu)}\int_0^{\infty}\exp[-u(t+z)]u^{\nu-1}\,du,\quad \mathrm{Re}\,\nu>0, \tag{15}$$

and

$$\frac{\ln(t+z)}{(t+z)^2}=\int_0^{\infty}\exp[-u(t+z)](1-C-\ln u)u\,du, \tag{16}$$

where $\Gamma(z)$ is the Euler gamma function, $C\simeq0.577216$ is the Euler-Mascheroni constant, and $z=\ln x$ [or $z=\ln(1-x)$]. Then for $\alpha_S(\lambda Q^2)$ we get

$$\alpha_S(\lambda Q^2)=\alpha_S t\int_0^{\infty}\exp(-ut)\lambda^{-u}R(u,t)du,$$

$$R(u,t)=1-\frac{\beta_1}{\beta_0^2}u(1-C-\ln t-\ln u). \tag{17}$$

After integration in Eq. (2) over x employing Eqs. (5) and (17) we find

$$[Q^2F_{M\gamma}(Q^2)]^{res}=\sqrt{3}Nf_{\pi}\Bigg\{\sum_{n=0}^{\infty}\frac{K_n}{n+1}+\frac{8}{3\beta_0}\int_0^{\infty}\exp(-ut)R(u,t)\sum_{n=0}^{\infty}K_n(B(2,1+n-u)$$
$$\times\{[\psi(1+n-u)-\psi(3+n-u)]^2+\psi'(1+n-u)-\psi'(3+n-u)+\psi(1+n-u)$$
$$-\psi(3+n-u)-9\}-B(1,2+n-u)[\psi(2+n-u)-\psi(3+n-u)])du\Bigg\}, \tag{18}$$

where $B(x,y)=\Gamma(x)\Gamma(y)/\Gamma(x+y)$ is the Beta function and $\psi(z)=d\ln\Gamma(z)/dz$. The second term in Eq. (18) is the inverse Borel transformation, the integrand in Eq. (18) without the exponential factor $\exp(-ut)$ is the Borel transform $B[Q^2F_{M\gamma}](u)$ of the series in Eq. (13). In deriving of the expression (18) we take into account that because of the symmetry of the η_1 and η_8 mesons DA's and T_H under replacement $x\leftrightarrow1-x$, the second term in Eq. (5) after integration over x leads to the same contribution as the first term.

The obtained result (18) is valid for all DA's of the mesons η_1,η_8. But we are going to use in our numerical calculations only two terms ($b_0,b_2\neq0$) from Eq. (7), therefore in Eq. (18) $n=0,1,2$ and the coefficients K_n in Eq. (9) are

$$K_0=1+6b_2(Q^2),\quad K_1=-30b_2(Q^2),\quad K_2=30b_2(Q^2). \tag{19}$$

It is evident that the divergence of the integral in Eq. (2) manifests itself as the divergence in the inverse Borel transformation (18). To reveal the nature of this divergence and outline a way for its regularization it is convenient to simplify the Borel transform $B[Q^2F_{M\gamma}](u)$ using the following formulas [24]:

$$\Gamma(1+z)=z\Gamma(z),\quad \psi(z+n)=\psi(z)+\sum_{k=0}^{n-1}\frac{1}{k+z},$$

$$\psi'(z+n)=\psi'(z)-\sum_{k=0}^{n-1}\frac{1}{(k+z)^2}. \tag{20}$$

Then after simple manipulations, for instance, for $n=0$, we get

$$B[Q^2F_{M\gamma}](u)|_{n=0}=R(u,t)\left[\frac{2}{(1-u)^3}-\frac{2}{(2-u)^3}-\frac{1}{(1-u)^2}+\frac{2}{(2-u)^2}-\frac{9}{(1-u)(2-u)}\right]. \tag{21}$$

The analysis fulfilled by taking into account also $n=1,2$ terms in Eq. (18) allows us to state that the inverse Borel transformation has a finite number of the triple, double, and single poles located at positive integers $u_0=1,2,3,4$ in the Borel plane. In other words, the inverse Borel transformation contains the infrared renormalon poles and some method has to be applied to remove them from Eq. (18). The possible prescriptions include deforming the integration contour in Eq. (18) into the complex plane so that it runs above the poles or below the poles. We adopt here the principal value prescription. The inverse Borel transformation after such regularization becomes the resummed form factor $[Q^2F_{M\gamma}(Q^2)]^{res}$.

The expression $[Q^2F_{M\gamma}(Q^2)]^{res}$ takes into account power suppressed corrections $\sim1/Q^p$, $p=2,4,6,\ldots$ to the form factor, which are implicitly contained in Eq. (18). To clarify this point let us calculate the $O(\alpha_S)$ correction to the form factor $Q^2F_{M\gamma}(Q^2)$ applying the infrared matching scheme [28]. For simplicity, let us choose a meson asymptotic DA (8). Then the correction is given by the formula

$$[Q^2F_{M\gamma}(Q^2)]_1=\frac{\sqrt{3}NC_Ff_M}{2\pi}\int_0^1\alpha_S(Q^2x)\times\left[\ln^2 x-\frac{x\ln x}{1-x}-9+\ln x\right](1-x)dx, \tag{22}$$

which can be expressed in terms of moment integrals $f_p(Q)$ defined as

$$f_p(Q)=\frac{p}{Q^p}\int_0^Q dk\, k^{p-1}\alpha_S(k^2). \tag{23}$$

Indeed, for the simplest term in Eq. (22) we have

$$F_p(Q)=\int_0^1\alpha_S(Q^2x)(1-x)dx=f_2(Q)-\frac{1}{2}f_4(Q). \tag{24}$$

After some manipulations, i.e., after changing in the integral the variable $x\rightarrow 1-y$, expanding ln$(1-y)$ as a power series in y and returning again to the variable x after $y\rightarrow 1-x$, we get

$$\int_0^1\alpha_S(Q^2x)(1-x)\ln x\; dx=\sum_{n=1}^{\infty}\frac{1}{n}\sum_{l=0}^{n+1}\frac{(-1)^{l+1}}{l+1}C_{n+1}^l f_{2(l+1)}(Q), \tag{25}$$

where C_{n+1}^l are the Newton binomial coefficients. Similar expressions can also be found for other terms in Eq. (22).

Now using the infrared matching scheme one can find the moment integrals $f_p(Q)$ as a sum of a nonperturbative and perturbative parts. For example, for the integral (24) we have

$$\int_0^1\alpha_S(Q^2x)(1-x)dx=\frac{\mu^2}{Q^2}f_2(\mu)-\frac{1}{2}\left(\frac{\mu^2}{Q^2}\right)^2 f_4(\mu)+\frac{\alpha_S}{2}[1-2\Gamma(1,2z)+\Gamma(1,4z)]+\frac{\alpha_S^2\beta_0}{16\pi}[3-4\Gamma(2,2z)+\Gamma(2,4z)]+\dots . \tag{26}$$

Here, $\alpha_S\equiv\alpha_S(Q^2)$, μ is the infrared matching scale, $z=\ln(Q/\mu)$, and $\Gamma(n+1,z)$ is the incomplete gamma function,

$$\Gamma(n+1,z)=\int_z^{\infty}e^{-t}t^n\,dt. \tag{27}$$

All the nonperturbative information is contained in the parameters $f_2(\mu)$ and $f_4(\mu)$, which represent weighted averages of α_S over the infrared region $0<k<\mu$. The resulting contribution to $F_p(Q)$ from the infrared region is a power correction of order $1/Q^p$, $p=2,4$.

After truncating the series like Eq. (25) at some $n=N$ and employing Eq. (24) one can separate the $O(\alpha_S)$ correction to the transition form factor $Q^2F_{M\gamma}(Q^2)$ into two parts; power suppressed corrections $\sim 1/Q^p$ and a perturbative contribution. In other words, the infrared matching scheme allows us to estimate power corrections to $F_{M\gamma}(Q^2)$ by explicitly dividing them from the full expression and introducing moment integrals $f_p(\mu)$ as new nonperturbative parameters. The values of the parameters $f_p(\mu)$ have to be deduced from experimental data. In the framework of the running coupling constant method we estimate the same power suppressed corrections to the form factor $F_{M\gamma}(Q^2)$, but here we do not need additional information on $f_p(\mu)$. In our previous work [29] we compared results for the pion electromagnetic FF $F_{\pi}(Q^2)$ obtained using these two methods with each other. They practically coincide, except for a region of small Q^2. In this paper we do not bring calculation of $F_{M\gamma}(Q^2)$ by means of the infrared matching scheme to numerical results, mainly owing to the lack of phenomenological information on $f_p(\mu)$, $p>2$. It is worth noting that values of nonperturbative parameters $f_p(\mu)$ calculated by means of the running coupling constant method

$$f_p(\mu)=p\frac{2\pi}{\beta_0}\frac{li(\lambda^{p/2})}{\lambda^{p/2}},\quad li(x)=\mathrm{P.V.}\int_0^x\frac{dt}{\ln t}, \tag{28}$$

where $\lambda=\mu^2/\Lambda^2$, $p=2,4,6,\dots$, are comparable with ones extracted from experimental data, when experimental values of $f_p(\mu)$ are available [29].

The principal-value prescription adopted in this paper to regularize the integral in Eq. (18) generates power suppressed (higher twist) ambiguities $\sim(\Lambda^2/Q^2)^q\Phi_q(Q^2)$, where $\Phi_q(Q^2)$ are calculable functions completely fixed by the residues of the Borel transform $B[Q^2F_{M\gamma}](u)$ at $u_0=q$, $q=1,2,3,4$. These ambiguities are canceled by ultraviolet renormalon ambiguities in the higher twist contributions to $F_{M\gamma}(Q^2)$. The crucial assumption (the ultraviolet dominance assumption) is that not only the ambiguity, but the whole higher twist contribution is proportional to $\Phi_q(Q^2)$. Hence Eq. (18) takes the form

$$[Q^2F_{M\gamma}(Q^2)]^{res}\Rightarrow[Q^2F_{M\gamma}(Q^2)]^{res}+\sum_{q=1}^{4}N_q\left(\frac{\Lambda^2}{Q^2}\right)^q\Phi_q(Q^2), \tag{29}$$

where N_q are arbitrary constants. The constants N_q and their sign have to be fixed from experimental data.

IV. η AND η' MESONS ELECTROMAGNETIC TRANSITION FORM FACTORS

In this section we calculate the η and η' mesons transition FF's $F_{\eta\gamma}(Q^2)$ and $F_{\eta'\gamma}(Q^2)$ within the ordinary $\eta-\eta'$ mixing scheme using the result for $F_{M\gamma}(Q^2)$ obtained in Sec. III. It is easy to demonstrate that in the ordinary η

$-\eta'$ mixing scheme the relations between $SU_f(3)$ basis states η_1, η_8 and the physical ones η, η' [Eq. (1)] lead to the similar relations between the physical transition form factors and $\eta_1\gamma, \eta_8\gamma$ form factors

$$F_{\eta\gamma}(Q^2) = \cos\theta F_{\eta_8\gamma} - \sin\theta F_{\eta_1\gamma}(Q^2),$$
$$F_{\eta'\gamma}(Q^2) = \sin\theta F_{\eta_8\gamma} + \cos\theta F_{\eta_1\gamma}(Q^2). \tag{30}$$

In the literature [10–16] the different values for θ were predicted. Thus from the phenomenological analysis of various decay processes and of $\pi^- p$ scattering $\theta \simeq -20°$ was found [10], whereas a similar consideration fulfilled by including constituent quark mass effects [11] gave $\theta = -14° \pm 2°$. At the leading order in the chiral perturbation theory (ChPT) by diagonalizing the η and η' mass matrix the value $\theta = -10°$ was obtained. The $O(p^4)$ order corrections [12] considerably change the lowest-order ChPT result and yield $\theta = -20°$. In this work we rely on the recent phenomenological analysis carried out in Ref. [16] and use in numerical calculations the following values of f_1, f_8, and θ:

$$f_1 = 1.17 f_\pi \simeq 0.108\ \text{GeV}, \quad f_8 = 1.26 f_\pi \simeq 0.116\ \text{GeV},$$
$$\theta = -15.4°, \tag{31}$$

where $f_\pi = 0.0923$ GeV is the pion decay constant.

The expressions (30) determine also the asymptotic behavior of the $\eta\gamma$ and $\eta'\gamma$ transition form factors. Since, for $Q^2 \to \infty$, any distribution amplitude (7) evolves into the asymptotic one,

$$\phi_M(x,Q^2) \to \sqrt{3} f_M x(1-x), \tag{32}$$

the model-independent limits of the form factors are

$$Q^2 F_{\eta(\eta')\gamma}(Q^2) \to 4\sqrt{\frac{2}{3}} f^1_{\eta(\eta')} + \frac{2}{\sqrt{3}} f^8_{\eta(\eta')}. \tag{33}$$

The decay constants $f^i_{\eta(\eta')}$, $i = 1,8$ in the usual flavor octet-singlet mixing scheme read

$$f^8_\eta = f_8 \cos\theta, \quad f^1_\eta = -f_1 \sin\theta,$$
$$f^8_{\eta'} = f_8 \sin\theta, \quad f^1_{\eta'} = f_1 \cos\theta. \tag{34}$$

Then, using the values of the parameters f_1, f_8, and θ from Eq. (31), we obtain

$$Q^2 F_{\eta\gamma}(Q^2)|_{Q^2\to\infty} \simeq 0.223\ \text{GeV},$$
$$Q^2 F_{\eta'\gamma}(Q^2)|_{Q^2\to\infty} \simeq 0.304\ \text{GeV}. \tag{35}$$

In Refs. [15] and [16] the new and general parametrization, i.e., the two-angle mixing scheme

$$f^8_\eta = f_8 \cos\theta_8, \quad f^1_\eta = -f_1 \sin\theta_1,$$
$$f^8_{\eta'} = f_8 \sin\theta_8, \quad f^1_{\eta'} = f_1 \cos\theta_1, \tag{36}$$

has been adopted and on the basis of the theoretical and phenomenological analyses two parameter sets have been proposed [16]:
Theory,

$$\text{(I)} \quad f_1 = 1.15 f_\pi \simeq 0.106\ \text{GeV}, \quad f_8 = 1.28 f_\pi \simeq 0.118\ \text{GeV},$$
$$\theta_1 = -2.7°, \quad \theta_8 = -21.0°; \tag{37}$$

phenomenology,

$$\text{(II)} \quad f_1 = 1.17 f_\pi \simeq 0.108\ \text{GeV}, \quad f_8 = 1.26 f_\pi \simeq 0.116\ \text{GeV},$$
$$\theta_1 = -9.2°, \quad \theta_8 = -21.2°. \tag{38}$$

For these parameters the $Q^2 \to \infty$ limits (33) of the form factors are

$$\text{(I)} \quad Q^2 F_{\eta\gamma}(Q^2)|_{Q^2\to\infty} \simeq 0.141\ \text{GeV},$$
$$Q^2 F_{\eta'\gamma}(Q^2)|_{Q^2\to\infty} \simeq 0.297\ \text{GeV},$$
$$\text{(II)} \quad Q^2 F_{\eta\gamma}(Q^2)|_{Q^2\to\infty} \simeq 0.182\ \text{GeV},$$
$$Q^2 F_{\eta'\gamma}(Q^2)|_{Q^2\to\infty} \simeq 0.30\ \text{GeV}. \tag{39}$$

The $\eta\gamma$ and $\eta'\gamma$ transition form factors calculated employing the η_1 and η_8 mesons asymptotic DA's and the different parameter sets from Eqs. (31), (37), (38) are shown in Fig. 1. For the $\eta'\gamma$ transition form factor all three sets give approximately the same results. But the $\eta\gamma$ transition form factors obtained using I and II parameter sets are in conflict with the data. The disagreement is dramatic for the I set, arising from the too low value of the mixing angle $|\theta_1|$. The two-angle mixing scheme and the corresponding parameter set applied for calculation of the $\eta\gamma$ and $\eta'\gamma$ transition form factors in the context of the modified HSA led to good description of the experimental data [15]. But this scheme and the parameter sets I and II seem not acceptable in our case. Within the RCC method the reliable parameter set is one from Eq. (31). In what follows we use the usual octet-singlet mixing scheme and this set of parameters.

It is interesting to clarify the dependence of the form factors (at fixed f_1, f_8) on the value θ. The η_1 and η_8 mesons asymptotic DA's (8) with the decay constants f_1, f_8, and θ from Eq. (31) give the $\eta\gamma$ form factor that may be considered as describing the data [Fig. 2(a)] and $Q^2 F_{\eta'\gamma}(Q^2)$ lying below the corresponding data [Fig. 2(b)] excluding some points. By varying the value of θ at fixed f_1, f_8 we observe that at θ smaller than $\theta = -15.4°$ the situation with $F_{\eta\gamma}(Q^2)$ becomes better, whereas $F_{\eta'\gamma}(Q^2)$ decreases with decreasing of θ. At θ larger than $\theta = -15.4°$ we find the opposing picture (it is not shown in Fig. 2).

To make the quantitative conclusions concerning the form factors at various values of Q^2, θ, b_2 it is convenient to introduce the ratio

$$R_M(Q^2,\theta,b_2) = \frac{F_{M\gamma}(Q^2,\theta,b_2) - F_{M\gamma}(Q^2,\tilde{\theta},\tilde{b}_2)}{F_{M\gamma}(Q^2,\theta,b_2)}. \tag{40}$$

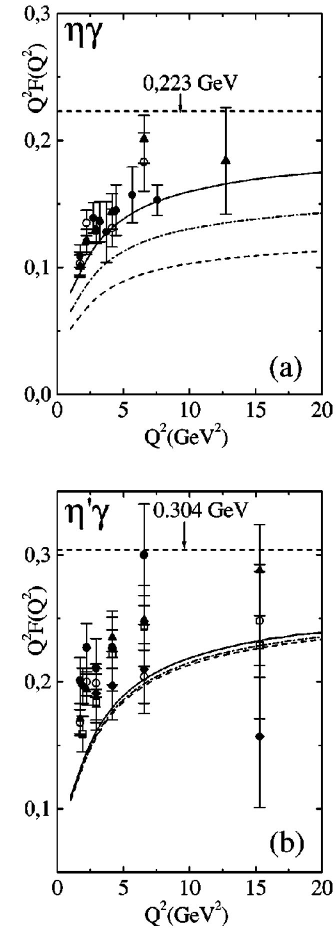

FIG. 1. The $\eta\gamma$ (a) and $\eta'\gamma$ (b) electromagnetic transition form factors vs Q^2. In calculations the η_1 and η_8 mesons asymptotic DA's are used. The solid curves correspond to the parameter set (31), the dashed curves to the parameter set I (37), the dot-dashed curves to the parameter set II (38). The upper dashed lines demonstrate the model-independent limits of the corresponding form factors (35). The data are taken from Ref. [8].

Then at $b_2^0=\tilde{b}_2^0\equiv 0$ and $\theta=-20°,\tilde{\theta}=-15.4°$ we get

$$R_{\eta}(2{,}23\ \mathrm{GeV}^2,-20°)\simeq 0.096,$$

$$R_{\eta}(10\ \mathrm{GeV}^2,-20°)\simeq 0.096,$$

$$R_{\eta}(20\ \mathrm{GeV}^2,-20°)\simeq 0.097,$$

and for $\theta=-22°,\tilde{\theta}=-15.4°$ we find

$$R_{\eta}(2{,}23\ \mathrm{GeV}^2,-22°)\simeq 0.098,$$

$$R_{\eta}(10\ \mathrm{GeV}^2,-22°)\simeq 0.13,$$

$$R_{\eta}(20\ \mathrm{GeV}^2,-22°)\simeq 0.13.$$

In the case of the η' meson we have

(i) $b_2^0=\tilde{b}_2^0\equiv 0$ and $\theta=-20°,\tilde{\theta}=-15.4°$,

$$R_{\eta'}(2{,}23\ \mathrm{GeV}^2,-20°)\simeq -0.066,$$

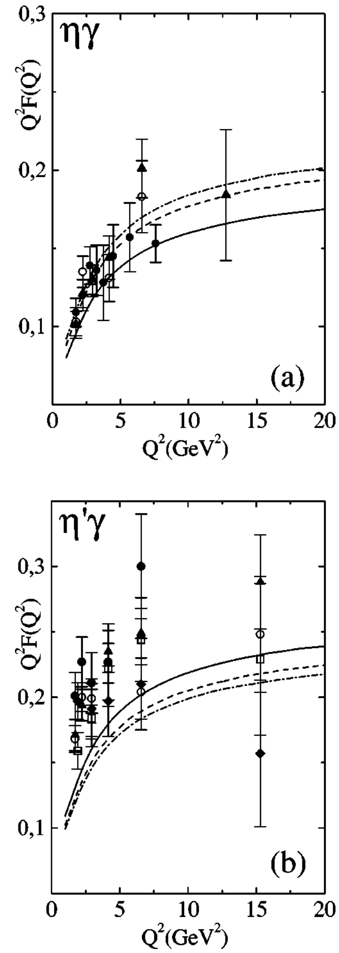

FIG. 2. The $\eta\gamma$ (a) and $\eta'\gamma$ (b) electromagnetic transition form factors vs Q^2. All curves are obtained employing the asymptotic DA's for both the η_1 and η_8 mesons. The solid curves correspond to the octet-singlet mixing angle $\theta=-15.4°$, the dashed curves to $\theta=-20°$, the dot-dashed curves to $\theta=-22°$.

$$R_{\eta'}(10\ \mathrm{GeV}^2,-20°)\simeq -0.067,$$

$$R_{\eta'}(20\ \mathrm{GeV}^2,-20°)\simeq -0.065,$$

(ii) $\theta=-22°,\tilde{\theta}=-15.4°$,

$$R_{\eta'}(2{,}23\ \mathrm{GeV}^2,-22°)\simeq -0.098,$$

$$R_{\eta'}(10\ \mathrm{GeV}^2,-22°)\simeq -0.1,$$

$$R_{\eta'}(20\ \mathrm{GeV}^2,-22°)\simeq -0.098.$$

As is seen, the ratio R is stable in all cases, but the $\eta\gamma$ form factor is more sensitive to θ than the $\eta'\gamma$ one.

The small admixture of the Gegenbauer polynomial $C_2^{3/2}(2x-1)$ in the DA of the η_1 meson and the η_8 meson asymptotic DA leads to better agreement with the data than two asymptotic DA's. In Fig. 3 the $\eta\gamma$ and $\eta'\gamma$ form factors calculated using the η_8 meson asymptotic and the η_1 meson model DA's are shown. For both $\eta\gamma$ and $\eta'\gamma$ FF's the difference between curves with various b_2^0 is mild in the domain

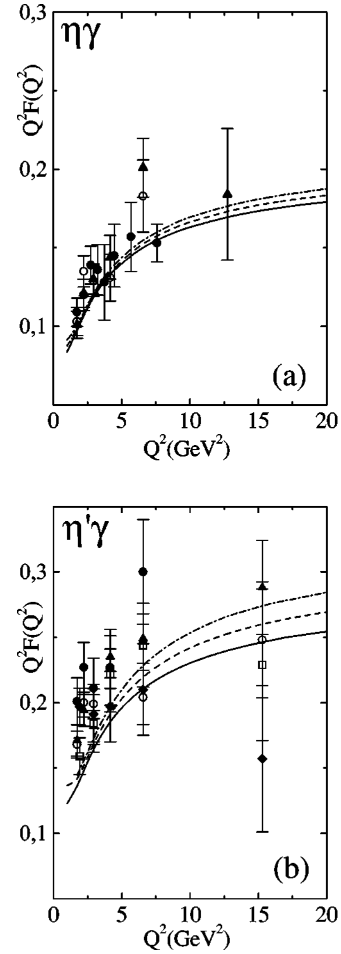

FIG. 3. The $\eta\gamma$ (a) and $\eta'\gamma$ (b) transition form factors as functions of Q^2. The octet-singlet mixing angle is $\theta=-15.4°$. All curves are calculated using the asymptotic DA for the η_8 meson. The correspondence between the curves and DA of the η_1 meson is: the solid curves $b_2^0=0.05$, the dashed curves $b_2^0=0.1$, the dot-dashed curves $b_2^0=0.15$.

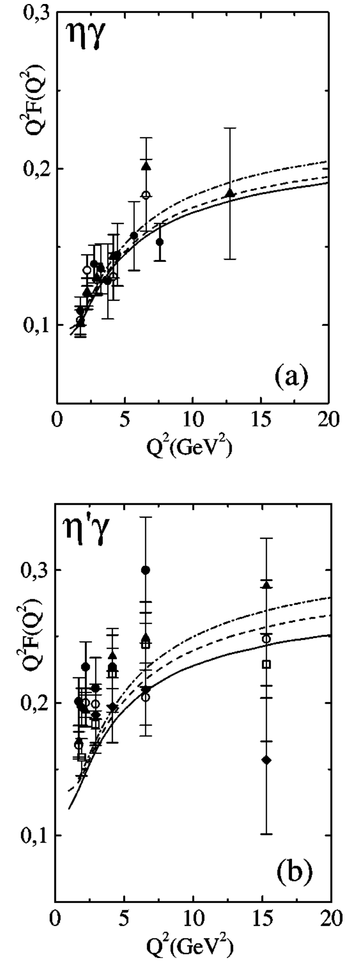

FIG. 4. The $\eta\gamma$ (a) and $\eta'\gamma$ (b) transition form factors at fixed $\theta=-15.4°$. The correspondence between the curves and the parameters of the η_1 and η_8 mesons model DA's is: the solid curves $b_2^0(\eta_1)=0.05, b_2^0(\eta_8)=0.1$; the dashed curves $b_2^0(\eta_1)=0.1, b_2^0(\eta_8)=0.1$; the dot-dashed curves $b_2^0(\eta_1)=0.15, b_2^0(\eta_8)=0.15$.

of small Q^2 and becomes significant at large Q^2. Indeed, for the ratio R_η at $Q^2=6.56\ \mathrm{GeV}^2$ we have

$$R_\eta(6.56\ \mathrm{GeV}^2, b_2^0=0.05) = \frac{F_{\eta\gamma}(6.56\ \mathrm{GeV}^2, 0.05) - F_{\eta\gamma}(6.56\ \mathrm{GeV}^2, 0)}{F_{\eta\gamma}(6.56\ \mathrm{GeV}^2, 0.05)} \simeq 0.017,$$

and at $Q^2=20\ \mathrm{GeV}^2$ $R_\eta(20\ \mathrm{GeV}^2, b_2^0=0.05)\simeq 0.023$. The same ratio for the $\eta'\gamma$ form factor is $R_{\eta'}(5\ \mathrm{GeV}^2, b_2^0=0.05)\simeq 0.036, R_{\eta'}(20\ \mathrm{GeV}^2, b_2^0=0.05)\simeq 0.06$. Increasing b_2^0 in the η_1 meson DA we increase the $\eta\gamma$ and $\eta'\gamma$ form factors. Thus $R_\eta(6.56\ \mathrm{GeV}^2, b_2^0=0.15)\simeq 0.047$, $R_\eta(20\ \mathrm{GeV}^2, b_2^0=0.15)\simeq 0.067$ and $R_{\eta'}(5\ \mathrm{GeV}^2, b_2^0=0.15)\simeq 0.1, R_{\eta'}(20\ \mathrm{GeV}^2, b_2^0=0.15)\simeq 0.16$. As is seen, the considering effect is impressive for the $\eta'\gamma$ form factor. This is understandable, because the η' dominantly consists of the η_1 meson. We have also studied transition form factors choosing the model DA's ($b_2^0\neq 0$) for the η_8 meson and asymptotic DA for η_1 and have found that the $\eta'\gamma$ form factor is less sensitive to b_2^0 than in the first case.

In Fig. 4 the form factors obtained using the model DA's with $b_2^0\neq 0$ for both $\eta_1$and η_8 mesons are plotted. Again the agreement with the data is better for the $\eta\gamma$ form factor than for the $\eta'\gamma$ one. Nevertheless, we can state that the η_1 and η_8 model DA's with $b_2^0=0.1$–0.15 describe the experimental data on the $\eta\gamma, \eta'\gamma$ transition form factors.

In Figs. 3 and 4 the form factors found by neglecting the evolution of the meson distribution amplitude $\phi_M(x,Q^2)$ on the scale Q^2 $[\phi_M(x,Q^2)=\phi_M(x,\mu_0^2)]$ are depicted. The effect of the evolution of the η_1,η_8 mesons DA's on the $\eta\gamma$ and $\eta'\gamma$ transition form factors does not exceed 2% at $Q^2=5\ \mathrm{GeV}^2$ and 5% at $Q^2=20\ \mathrm{GeV}^2$ (Fig. 5, curves 1). In these computations the normalization point μ_0 has been taken equal to 1 GeV and the anomalous dimension is $\gamma_2=50/9$.

The higher twist corrections to the form factors are shown in Fig. 6. Since the constants N_q and their sign are free

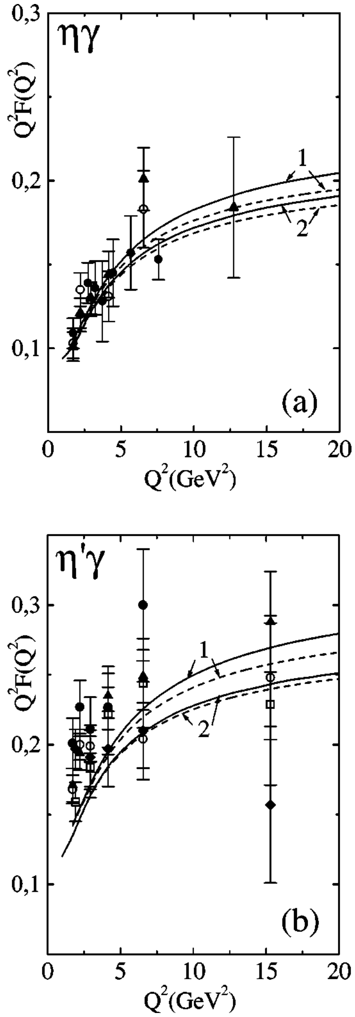

FIG. 5. Results for the $\eta\gamma$ (a) and $\eta'\gamma$ (b) transition form factors obtained using the η_1 and η_8 mesons model DA's with the parameters $b_2^0(\eta_1)=b_2^0(\eta_8)=0.15$ (curves 1) and $b_2^0(\eta_1)=0.05, b_2^0(\eta_8)=0.1$ (curves 2). The solid (dashed) curves are found by neglecting (by taking into account) the evolution of the DA's on the factorization scale Q^2.

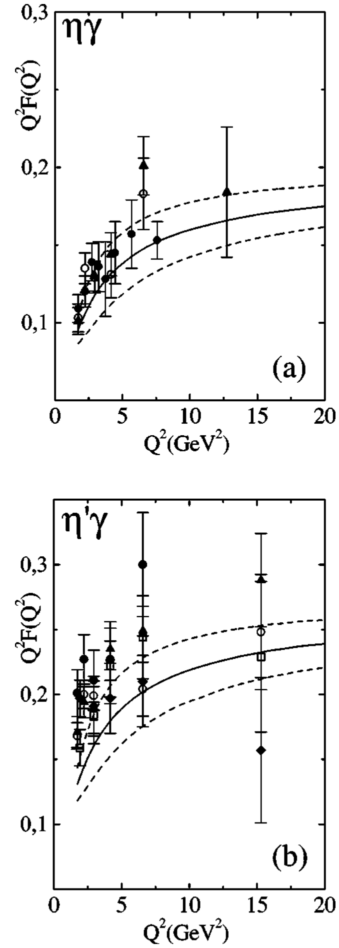

FIG. 6. Higher twist contributions to the $\eta\gamma$ (a) and $\eta'\gamma$ (b) transition form factors. In computations the η_1 and η_8 mesons asymptotic DA's are employed. The solid curves are the form factors within the RCC method (18). The upper dashed curves correspond to $N_1=N_2=1$, the lower ones to $N_1=N_2=-1$ [see Eq. (29)].

parameters, in the simple case of the asymptotic DA's we have examined two possibilities: $N_1=N_2=1$ and $N_1=N_2=-1$. These corrections do not exceed $\pm 15\%$ of the corresponding form factors.

V. CONCLUSIONS

In this work we have calculated the $\eta\gamma$ and $\eta'\gamma$ electromagnetic transition form factors in the standard HSA and usual mixing scheme applying the running coupling constant method. We have demonstrated that the conventional mixing scheme with $SU_f(3)$ octet-singlet mixing angle $\theta=-15.4°$ and η_1, η_8 mesons model DA's including the small admixture of the Gegenbauer polynomial $C_2^{3/2}(2x-1)$ lead to the $\eta\gamma$ and $\eta'\gamma$ electromagnetic transition form factors, which are in agreement with the experimental data in a range of the virtuality of the probing photon, $1.5 \leq Q^2 \leq 15$ GeV^2. We have estimated the coefficients b_2^0 in Eq. (7) as $b_2^0=0.1$–0.15 for both η_1 and η_8 mesons, but even the asymptotic DA's are not in evident conflict with the data. We have also examined within the RCC method the two-angle mixing scheme [15,16] and found that the parameter sets proposed in Ref. [16] do not describe the data on the $\eta\gamma$ transition form factor, mainly due to a small value of the mixing angle $|\theta_1|$.

We have taken into account the evolution of the model DA's on the factorization scale Q^2 and found that its effect on the form factors in the considering range of Q^2 is small (5% at $Q^2=20$ GeV^2). The higher twist corrections to $Q^2F_{\eta(\eta')\gamma}(Q^2)$ estimated applying the ultraviolet dominance assumption do not exceed $\pm 15\%$ of the corresponding form factors.

In our investigations of $Q^2F_{\eta(\eta')\gamma}(Q^2)$ the intrinsic gluon and charm components of the η and η' mesons have been neglected. It is quite possible that their consideration will improve an agreement of our results with the experimental data. But these problems require further studies.

[1] G. P. Lepage and S. J. Brodsky, Phys. Rev. D **22**, 2157 (1980).
[2] A. V. Efremov and A. V. Radyushkin, Phys. Lett. **94B**, 245 (1980); A. Duncan and A. H. Mueller, Phys. Rev. D **21**, 1636 (1980).
[3] V. L. Chernyak and A. R. Zhitnitsky, Phys. Rep. **112**, 173 (1984).
[4] G. Sterman and P. Stoler, Annu. Rev. Nucl. Part. Sci. **47**, 193 (1997).
[5] F. del Aguila and M. K. Chase, Nucl. Phys. **B193**, 517 (1981).
[6] E. Braaten, Phys. Rev. D **28**, 524 (1983).
[7] E. P. Kadantseva, S. V. Mikhailov, and A. V. Radyushkin, Yad. Fiz. **44**, 507 (1986) [Sov. J. Nucl. Phys. **44**, 326 (1986)].
[8] CLEO Collaboration, J. Gronberg *et al.*, Phys. Rev. D **57**, 33 (1998).
[9] CELLO Collaboration, H.-J. Behrend *et al.*, Z. Phys. C **49**, 401 (1991).
[10] F. J. Gilman and R. Kauffman, Phys. Rev. D **36**, 2761 (1987).
[11] A. Bramon and M. D. Scadron, Phys. Lett. B **234**, 346 (1990).
[12] E. P. Venugopal and Barry R. Holstein, Phys. Rev. D **57**, 4397 (1998).
[13] J. Cao, F.-G. Cao, T. Huang, and B.-Q. Ma, Phys. Rev. D **58**, 113006 (1998).
[14] R. Jakob, P. Kroll, and M. Raulfs, J. Phys. G **22**, 45 (1996).
[15] Th. Feldmann and P. Kroll, Eur. Phys. J. C **5**, 327 (1998).
[16] Th. Feldmann, P. Kroll, and B. Stech, Phys. Rev. D **58**, 114006 (1998).
[17] S. J. Brodsky, T. Huang, and G. P. Lepage, in *Particles and Fields-2*, Proceedings of the Banff Summer Institute, Banff, Alberta, 1981 (Plenum, New York, 1983).
[18] M. Beneke, Phys. Rep. **317**, 1 (1999).
[19] S. S. Agaev, Phys. Lett. B **360**, 117 (1995); **369**, 379(E) (1996); Mod. Phys. Lett. A **10**, 2009 (1995); **11**, 957 (1996).
[20] S. S. Agaev, A. I. Mukhtarov, and Y. V. Mamedova, Mod. Phys. Lett. A **15**, 1419 (2000).
[21] P. Gosdzinsky and N. Kivel, Nucl. Phys. **B521**, 274 (1998).
[22] M. K. Chase, Nucl. Phys. **B174**, 109 (1980); M. V. Terentyev, Yad. Fiz. **33**, 1692 (1981) [Sov. J. Nucl. Phys. **33**, 911 (1981)]; V. N. Baier and G. Grozin, Nucl. Phys. **B192**, 476 (1981).
[23] S. J. Brodsky, G. P. Lepage, and P. B. Mackenzie, Phys. Rev. D **28**, 228 (1983).
[24] A. Erdelyi, *Higher Transcendental Functions* (McGraw-Hill, New York, 1953), Vols. 1 and 2.
[25] H. Contopanagos and G. Sterman, Nucl. Phys. **B419**, 77 (1994).
[26] G. 't Hooft, in *The Whys of Subnuclear Physics*, Proceedings of the International School, Erice, 1977, edited by A. Zichichi (Plenum, New York, 1978); V. I. Zakharov, Nucl. Phys. **B385**, 452 (1992).
[27] A. Erdelyi, *Tables of Integral Transforms* (McGraw-Hill, New York, 1954), Vol. 1.
[28] B. R. Webber, J. High Energy Phys. **10**, 012 (1998).
[29] S. S. Agaev, Nucl. Phys. B (Proc. Suppl.) **74**, 155 (1999).